Long-range correlations of density fluctuations in the Kerner-Klenov-Wolf cellular automata three-phase traffic flow model

J. J. Wu, H. J. Sun,* and Z. Y. Gao†
School of Traffic and Transportation, Beijing Jiaotong University, Beijing 100044, China
(Received 21 April 2008; published 3 September 2008)

Detrended fluctuation analysis (DFA) is a useful tool to measure the long-range power-law correlations in $1/f$ noise. In this paper, we investigate the power-law dynamics behavior of the density fluctuation time series generated by the famous Kerner-Klenov-Wolf cellular automata model in road traffic. Then the complexities of spatiotemporal, average speed, and the average density have been analyzed in detail. By introducing the DFA method, our main observation is that the free flow and wide moving jam phases correspond to the long-range anticorrelations. On the contrary, at the synchronized flow phase, the long-range correlated property is observed.

DOI: 10.1103/PhysRevE.78.036103 PACS number(s): 89.40.−a, 05.40.−a, 05.60.−k

INTRODUCTION

Traffic flow phenomena have attracted the interest of physicists since the early 1990s. How to accurately and realistically predict road traffic flow has become a hot topic in traffic works. Additionally, many traffic phenomena on the roads are complex and nonlinear, such as cluster formation, huge fluctuations, long-range dependencies, and so on. Thus, traffic models are developed to get a better understanding of these phenomena and how to avoid some problems caused by traffic congestion.

This paper is devoted to a theoretical analysis of the time scale of fluctuations in traffic flow. In 1976, Mush and Higuchi [1] found $1/f$ fluctuations in empirical data measured in traffic flow. There are many theoretical studies of fluctuations in traffic flow, which try to explain Mush and Higuchi's results as well as other empirical results about traffic flow fluctuations (see [2–7], and references therein). All these theoretical studies have been made in the context of the so-called fundamental diagram approach to traffic flow theory. However, as explained in [8] based on empirical analyses of spatiotemporal measured traffic data, this approach as well as related traffic flow models used in [2–7] cannot show and predict traffic breakdown and many important empirical features of resulting spatiotemporal congested patterns. For this reason, in a theoretical analysis of large time-scale fluctuations in traffic flow presented in this paper we use the Kerner-Klenov-Wolf (KKW) cellular automata (CA) traffic flow model in the framework of Kerner's three-phase traffic theory that explains and predicts empirical traffic breakdown and resulting congested patterns observed in real traffic. In this theory, there are three traffic phases: free flow, synchronized flow, and wide moving jams. As shown in [8], phase transitions between these phases determine the complexity of empirical spatiotemporal phenomena in real traffic. Thus we can expect that qualitatively different time scales of fluctuations should be associated with the three traffic phases.

Long-range correlated time series have been widely used for the theoretical description of diverse phenomena. There exist three long-range correlated processes including antipersistent, persistent, and ordinary diffusion. An antipersistent long-range correlated process shows that a step in one direction is preferentially followed by a reversal of direction. A persistent long-range correlated process indicates that a step in one direction is preferentially followed by another step in the same direction. While in the ordinary diffusion (random walk) process, each step is independent of its preceding one [9].

Indeed, the existence of power-law fluctuations in traffic flow has been discussed previously ([6,7], and references therein), which can be used to characterize the complex architectures of vehicle traffic. As mentioned above, the complex behaviors in the different traffic phases, such as the free flow phase, the synchronized flow phase, and the wide moving jam phase, also remain unknown. Therefore, the purpose of this paper is to investigate the large time-scale behavior of road traffic. We analyze the traffic flow under different densities and observe the density fluctuation characteristic by introducing the KKW model. Applying the detrended fluctuation analysis (DFA) method, we discuss the long-range correlated property hidden in this raw data of the traffic flow.

The paper is organized as follows. In Sec. II, we describe the method of detrended fluctuation analysis. In Sec. III, we review the KKW–1 cellular automata model. Simulation results are given in Sec. IV and a conclusion is offered in Sec. V.

DETRENDED FLUCTUATION ANALYSIS

Due to strong interactions among elements in the complex systems, long-range spatial and/or temporal correlations are often generated. These systems are then referred to as scale-free. An important feature of such systems is the power-law scaling behavior, which indicates the rather robust or universal properties [10].

DFA is a well-established method for determining data scaling behavior in the presence of possible trends without knowing their origin and shape [11,12]. Therefore, it is one of the methods used for analyzing a nonstationary time series with power-law properties. It was first developed for analyzing the long-range correlation in deoxyribonucleic acid se-

*sunhuijun@jtys.bjtu.edu.cn
†gaoziyou@jtys.bjtu.edu.cn

quences. Moreover, long-range correlation processes present very long-term fluctuations in addition to very short-term fluctuations, where the dependence of data farther apart is higher than is expected for independent data [13]. DFA avoids the spurious detection of correlations that are artifacts of nonstationarity which often affects experimental data. Such trends have to be well distinguished from the intrinsic fluctuations of the system in order to find the correct scaling behavior of the fluctuations. Very often the reasons for underlying trends in collected data are unknown and the scales of the underlying trends are also unknown.

The simplest form of the DFA method is described as follows. The methodology operates on the time series $\{h(t)\}$, $t=1,2,\ldots,T$, where T is the length of the time series. First the profile $y(t)$ of the time series is defined as the accumulated deviation from the mean,

$$y(t)=\sum_{i=1}^{t}[h(i)-\langle h\rangle], \tag{1}$$

where $\langle h\rangle=T^{-1}\Sigma_{t=1}^{T}h(t)$ is the mean value of the time series $\{h(t)\}$.

Then, the entire time series of the profile $y(t)$ of length T is divided into int(T/l) nonoverlapping segments of equal length l. The local trend $\tilde{y}_m(t)$ in the mth segment is defined by fitting the raw profile $y(t)$ in the segment. Here we employ the first order DFA method, where the linear least square method is used to fit the profile $y(t)$.

The detrended profile $y_l(t)$ is defined as the deviation of the original profile $y(t)$ from the local trend $\tilde{y}_m(t)$, then if $ml\leqslant t<(m+1)l$, we can derive

$$y_l(t)=y(t)-\tilde{y}_m(t). \tag{2}$$

Thus, the standard deviation of the detrended series is defined as the mean square of the detrended profile,

$$F^2(l)=T^{-1}\sum_{t=1}^{T}y_l^2(t). \tag{3}$$

By analyzing the dependence of the standard deviation $F(l)$ on the segment length l, we find the long-range correlation in the nonstationary time sequences. If the standard deviation $F(l)$ behaves as a power of the segment length l, $F(l)\sim l^{\alpha}$. If $0<\alpha<0.5$, $h(t)$ is long-range anticorrelated; if $0.5<\alpha<1.0$, it is called long-range correlated. $\alpha=0.5$ corresponds to the Gaussian white noise, while $\alpha=1.0$ indicates the $1/f$ noise.

KKW–1 CELLULAR AUTOMATA MODEL

Cellular automata are agent-based simulations for complex natural systems containing large numbers of simple identical components which interact locally. Recently, Kerner found that there are two different phases in congested traffic: synchronized flow and wide moving jam [14]. This distinguishment is based on the qualitatively different empirical spatiotemporal features of these phases. Thus, there are three traffic phases in the real traffic phenomena: (1) free flow; (2) synchronized flow; and (3) wide moving jam.

In order to explain these three phases, Kerner introduced a three-phase traffic theory [14]. One of the microscopic traffic flow models in the framework of Kerner's three-phase traffic theory is a cellular automata three-phase traffic flow model first proposed by Kerner, Klenov, and Wolf called the KKW CA model [15]. Because the KKW CA model can explain and predict measured spatiotemporal features of phase transitions and resulting congestion patterns, we use the simulation results obtained by the KKW-1 CA model for our analysis of the density fluctuation time series. The basic updated rules of the KKW-1 CA model including the deterministic part and the stochastic part are as follows [15]:

(1) Deterministic rule $(t<t_1<t+1)$

$$v_n(t_1)=\max\{0,\min\{v_{\max},v_{s,n}(t),v_{\mathrm{des}}(t)\}\}, \tag{4}$$

where v_n and $v_{\max}$ are the speed of nth car and the maximum speed of the vehicles. $v_{s,n}=d_n/\tau$ is the safe speed which must not be exceeded in order to avoid collisions (τ is the time discretization interval) and depends on the space gap between vehicles, $d_n=x_{j,n}-x_n-g$. The lower index j marks functions (or values) related to the vehicle in front of the one at x_n, the "leading vehicle," and g is the vehicle length (assumed to be the same for all vehicles in this paper). x_n denotes the position of vehicle n. $v_{\mathrm{des}}(t)$ is the expected speed at time t calculated by the following equation:

$$v_{\mathrm{des}}(t)=\begin{cases}v_n(t)+\theta\tau & \text{case 1} \quad (5)\\ v_n(t)+\theta\tau\Delta & \text{case 2}, \quad (5')\end{cases}$$

where $\Delta=\mathrm{sgn}[v_{n+1}(t)-v_n(t)]$, and case 1 and case 2 refer to $d_n>D[v_n(t)]-g$ and $d_n\leqslant D[v_n(t)]-g$, respectively. The function $\mathrm{sgn}(\varphi)$ is 1 for $\varphi>0$, 0 for $\varphi=0$, and -1 for $\varphi<0$. The vehicle will accelerate with θ when case 1 is satisfied. $D[v]$ denotes the synchronization distance calculated by $D[v]=D_0+kvt$, where D_0 and k are constants. This rule decouples speed and gaps between vehicles for dense traffic.

(2) Stochastic rule

$$v_{n+1}(t)=\max\{0,\min\{v_n(t_1)+\theta\tau\eta_n,v_n(t_1)+\theta\tau,v_{\max},v_{s,n}(t)\}\}. \tag{6}$$

The randomness item η_n is

$$\eta_n=\begin{cases}-1 & \text{if rand}(\,)<p_b \quad (7)\\ 1 & \text{if } p_b<\text{rand}(\,)<p_b+p_a \quad (7')\\ 0 & \text{otherwise}, \quad (7'')\end{cases}$$

where p_b and p_a are the probability of deceleration and acceleration determined by the current speed, respectively $(p_a+p_b\leqslant 1)$.

$$p_b(v_n)=\begin{cases}p_0 & \text{if } v_n=0 \quad (8)\\ \rho & \text{if } v_n>0, \quad (8')\end{cases}$$

where ρ and p_0 are constants $(p_0>\rho)$.

$$p_a(v_n)=\begin{cases}p_{a1} & \text{if } v_n<v_\rho \quad (9)\\ p_{a2} & \text{if } v_n\geqslant v_\rho, \quad (9')\end{cases}$$

where v_ρ, p_{a1}, and p_{a2} are constants $(p_{a1}<p_{a2})$. rand( ) is a random number uniformly distributed between 0 and 1. By setting the observing point in the road, we can calculate the

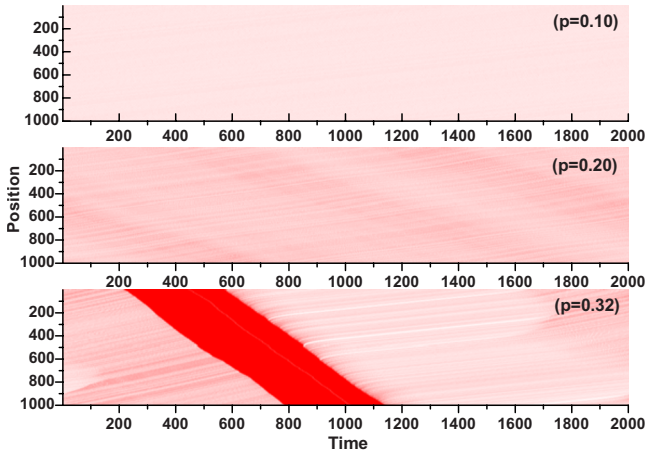

FIG. 1. (Color online) The spatiotemporal graph of free flow, synchronized flow, and wide moving jam on a homogeneous one lane road with periodic boundary conditions for the KKW–1 model. Free flow traffic phase is related to $p=0.1$, synchronized flow traffic phase is related to $p=0.2$, and wide moving jam traffic phase is related to $p=0.32$.

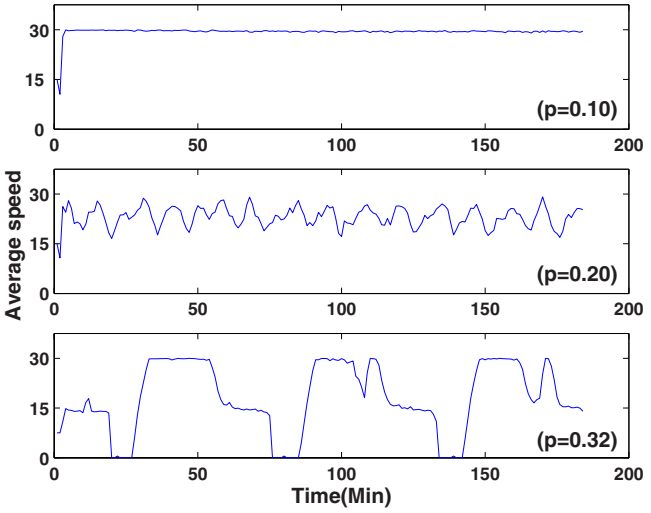

FIG. 2. (Color online) The average speed of free flow, synchronized flow, and wide moving jam on a homogeneous one lane road with periodic boundary conditions for the KKW–1 model. One minute averaged data of a virtual detector whose coordinates are indicated in the figure. Free flow traffic phase is related to $p=0.1$, synchronized flow traffic phase is related to $p=0.2$, and wide moving jam traffic phase is related to $p=0.32$.

average vehicle density $\bar{h}$ defined as the average speed divided by the total number of vehicles across the observing point. A detailed description and simulation condition can be found in the literature [15]. Additionally, the updated rule of vehicle position is

$$x_{n+1} = x_n + v_{n+1}(t+1)\tau. \tag{10}$$

SIMULATION RESULTS

In the KKW-1 CA model, the length of the cell is 0.5 m, the length of the road L is 30 000 m, each vehicle occupies 15 cells ($g=0.5\times 15=7.5$ m), and the maximum speed is $v_{\max}=108$ km/h$=60$ cells/s. The parameters $k=2.55$, $\tau=1$, $v_p=50.4$ km/h, $\rho=0.04$, $p_{a1}=0.2$, and $p_{a2}=0.052$, $\theta=0.5$ m/s^2 are given. Other parameters and variables are similar to the literature [15]. There is no on-ramp on the road, and the simulation is performed under periodic conditions. As the initial state, the positions of the vehicles are randomly chosen. The data is averaged over a one-minute time period in the paper. In order to analyze the results, the first 10 000 time steps of the simulation are discarded to let transients die out and the system reach its steady state. Assuming that the traffic is also considered to be homogeneous, all vehicle characteristics are assumed to be the same.

The spatiotemporal diagram is a graph that describes the relationship between the location of vehicles in a traffic stream and the time as the vehicles progress along the highway. Here, we give the spatiotemporal graph including free flow ($p=0.1$), synchronized traffic flow ($p=0.2$), and wide moving jam ($p=0.32$) in Fig. 1. The time and space axes are oriented from left to right, and top to bottom, respectively. Each dot corresponds to a vehicle at a given time step. One can observe that, for the low density (e.g., $p=0.1$), vehicles will arrive at the stable free flow states. With the increase of density, e.g., $p=0.2$, the synchronized flow traffic phases can be seen where the vehicle speed is lower than $v_{\max}$.

In general, traffic jams are characterized by a high local density and the low speed of the vehicles. From the view of observation, the wide moving jam is a localized structure moving upstream and is limited by two fronts where the vehicle speed changes sharply, i.e., within a region that is small compared to the distance between the fronts, while for the synchronized flow, the downstream front is usually fixed at the bottleneck, where it occurred. In particular, wide moving jams do not occur spontaneously, if the initial state with maximal vehicle speed $v=v_{\max}$ lies within the range of flow rates, where the maximal speed can be maintained [16]. Once the density is above a threshold for the moving jam formation, we can see the emergence of wide moving jams ($p=0.32$). At last, a wide congested band is formed. From Fig. 1, associated with $p=0.32$, we can see a backward movement of shock waves caused by the traffic jam.

Figure 2 shows the average speed for different densities $p=0.1$ (free flow), $p=0.2$ (synchronized flow), and $p=0.32$ (wide moving jam) by collecting the data from a virtual detector. Here, one minute averaged data is used. As can be seen, the average speed of free flow is steady and almost no fluctuations are observed. However, with the increase of density, the fluctuations of average speed become more and more obvious, which indicates the inhomogenous traffic in the system.

The next step is to analyze the time series of average density $\bar{p}$ obtained by setting the virtual detector in the road with different vehicle densities $p=0.05$, $p=0.1$, $p=0.2$, and $p=0.32$. As mentioned above, these density ranges correspond to the free flow ($p=0.05$ and $p=0.1$), synchronized flow ($p=0.2$), and wide moving jams ($p=0.32$) especially. Then, we report the time series of the density fluctuation curves in Fig. 3. One can see that, for a small p value, the

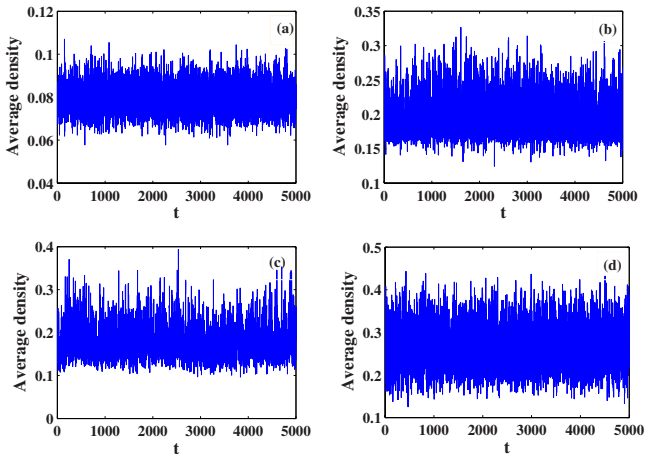

FIG. 3. (Color online) The time series of average density in the observing point for different initial vehicle densities: (a) free flow $p=0.05$; (b) free flow $p=0.1$; (c) synchronized flow $p=0.2$; and (d) wide moving jams $p=0.32$.

average density $\bar{p}$ fluctuates around an average value. In addition, the fluctuations are short ranged and small, which indicates short-range correlation; that is, the state of the system at a certain time step has very little effect on the state of the system a few time steps apart.

In Fig. 4, the DFA function calculated with $h(t)$ is displayed on a log-log scale. Clearly, the standard deviation F_l by using DFA on time series $h(t)$ exhibits the power-law form, and the exponent α in the free flow phase ($p=0.05$) is about 0.2621, while in the free flow phase related to $p=0.1$, the exponent α is about 0.3825. When $p=0.2$ and $p=0.32$, the phases of synchronized flow and wide moving jam will be displayed. Obviously, the power-law behaviors with one about $\alpha \approx 0.6513$ for synchronized flow and another about $\alpha \approx 0.4553$ for wide moving jam can be seen in Fig. 4. The calculated α value implies the long-range correlation for synchronized flow. However, for the free flow and wide moving jam, the scaling exponents calculated with DFA are long-

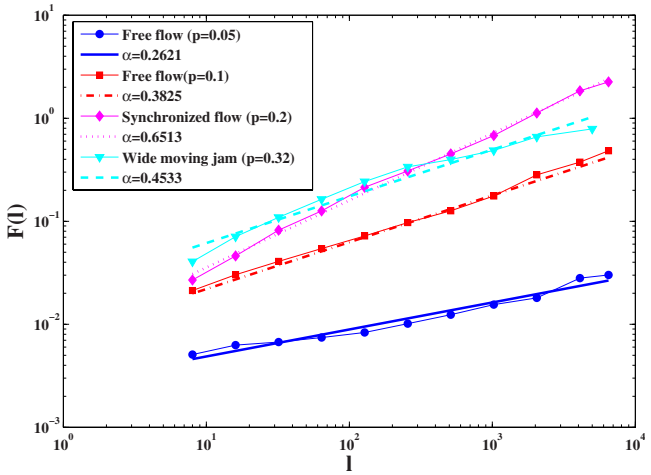

FIG. 4. (Color online) The detrended fluctuation analysis of the average density generated by the KKW–1 CA model (log-log graph). The different curves represent the cases of different initial vehicle density.

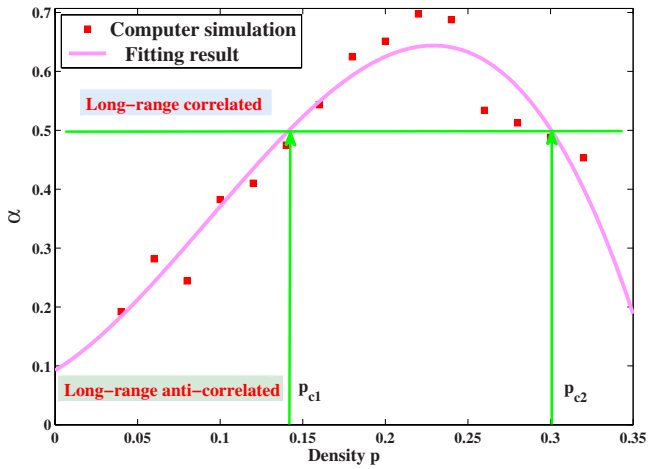

FIG. 5. (Color online) The calculated exponent α as a function of vehicle density p.

range and anticorrelated. The figure shows that the power-law behavior is really seen in the traffic system. In other words, long-range correlations in the traffic density fluctuation persist in the synchronized flow and are destroyed in the free flow and wide moving jam phases.

To study the correlated characteristics of density fluctuation in different cases, we give the relationship between the scaling exponent α and the vehicle density p in Fig. 5. Next, we show some critical results of the simulations. This diagram represents the fluctuation properties of the traffic flow as a function of density. It is clear that the diagram is divided into two parts by the black real line, long-range anticorrelated area under the line and long-range correlated area above the line. Additionally, two characteristic densities p, e.g., p_{c1} and p_{c2}, can be found. For $p<p_{c1}$ and $p>p_{c2}$, the exponent α lies in the long-range anticorrelated area. In the contrary, the long-range correlated property is displayed when $p_{c1} \leqslant p \leqslant p_{c2}$. As shown in Fig. 5, the exponent α exhibits approximately the Possion distribution. Both smaller and larger density, e.g., $p<0.145$ and $p>0.3$, the calculated exponent α shows that the raw data is long-range anticorrelated. However, when $0.145 \leqslant p \leqslant 0.3$, the long-range correlated behavior can be seen from the diagram.

CONCLUSION

In the empirical paper by Mush and Higuchi [1] in which $1/f$ noise in traffic flow has been observed, no spatiotemporal characteristics of traffic have been presented. Thus, based on Mush and Higuchi's analysis it is not possible to understand which traffic phase(s) is (are) responsible for $1/f$ noise. In this paper, we analyze the long-range correlation of density fluctuation in the KKW cellular automata three-phase traffic flow model by using the DFA method. It is found that the calculated α value implies the long-range correlation for synchronized flow. However, for the free flow and wide moving jam associated with the density $p=0.32$, the scaling exponent calculated with DFA shows the long-range anticorrelated behavior. Additionally, an interesting observation is that there exists a region of density $p_{c1} \leqslant p \leqslant p_{c2}$ in which the

time series are long-range correlated. We note, an empirical study of fluctuations in different traffic phases, i.e., separately in free flow, synchronized flow, and wide moving jam, could be an important task of further investigations.

ACKNOWLEDGMENTS

The authors wish to thank the anonymous referee for his/her helpful comments and suggestions for improvement. We also thank X.G. Li for the data and useful comments. This paper is partly supported by National Basic Research Program of China (Grant No. 2006CB705500), Fok Ying Tong Education Foundation (Grant No. 111083) and Foundation for the Author of National Excellent Doctoral Dissertation of China (Grant No. 200763).

[1] T. Musha and H. Higuchi, Jpn. J. Appl. Phys. **15**, 1271 (1976).
[2] S. Lübeck, M. Schreckenberg, and K. D. Usadel, Phys. Rev. E **57**, 1171 (1998).
[3] K. Nagel and M. Paczuski, Phys. Rev. E **51**, 2909 (1995).
[4] M. Takayasu and H. Takayasu, Fractals **1**, 860 (1993).
[5] X. Zhang and G. Hu, Phys. Rev. E **52**, 4664 (1995).
[6] S. Tadaki, M. Kikuchi, Y. Sugiyama, and S. Sugiyama, J. Phys. Soc. Jpn. **68**, 3110 (1999).
[7] L. Neubert, L. Santen, A. Schadschneider, and M. Schreckenberg, Phys. Rev. E **60**, 6480 (1999).
[8] B. S. Kerner, *The Physics of Traffic* (Springer, Berlin, 2004).
[9] S. M. Cai, G. Yan, T. Zhou, P. L Zhou, Z. Q. Fu, and B. H. Wang, Phys. Lett. A **366**, 14 (2007).
[10] C. P. Pan, B. Zheng, Y. Z. Wu, Y. Wang, and X. W. Tang, Phys. Lett. A **329**, 130 (2004).
[11] J. W. Kantelhardt, E. Konscienly-Bunde, H. H. A. Rego, S. Havlin, and A. Bunde, Physica A **295**, 441 (2001).
[12] L. Telesca, G. Colange, V. Lapenna, and M. Macchiato, Phys. Lett. A **332**, 398 (2004).
[13] M. Duarte and V. M. Zatsiorsky, Phys. Lett. A **283**, 124 (2001).
[14] B. S. Kerner, Phys. Rev. E **65**, 046138 (2002).
[15] B. S. Kerner, S. L. Klenov, and D. E. Wolf, J. Phys. A **35**, 9971 (2002).
[16] R. Jiang and Q. S. Wu, J. Phys. A **36**, 381 (2003).